Effect of Hull Vane on Wave Making Resistance of High-Speed Displacement Vessel

S Goutham[1], R Vijayakumar[2]

Department of Ocean Engineering, Indian Institute of Technology, Madras, India
Corresponding Authors. Email: [1]gouthamaarya9@gmail.com, [2]vijay2028@iitm.ac.in

Synopsis

Due to mandatory requirements Energy Efficiency Design Index (EEDI) and Energy Efficiency Existing Ship Index (EEXI)) prescribed by International Maritime Organisation (IMO) for new and existing ships, there is an increasing concern about the reducing the carbon emissions from the ships to have a sustainable environment. Several energy saving technologies are adopted to reduce fuel consumption and increase the efficiency of the ships. Since past two decades, high-speed crafts are fitted with different types of appendages for drag reduction such as stern flaps, stern wedges, trim tabs, and hull vanes. Amongst all the appendages, hull vane is found to be one of the suitable appendages at various Froude numbers (Fn 0.2 – 0.7). Hull vane is a fixed foil which is attached at the stern part of the vessel to improve the local pressure by altering the stern flow. This paper investigates the effect of the hull vane which is retrofitted to a high-speed Displacement vessel in 1:35 scale with different locations and angle of attack. Numerical study was carried out using Reynolds Averaged Navier Stokes equation (RANS) based Computational Fluid Dynamics (CFD) on Froude number ranges between 0.2 – 0.45. It has been found sinkage and trim has reduced significantly up to 20 percent along with the drag of the vessel in both theoretical and practical approach. For validating the present numerical study, towing tank experiments were carried out and compared. It was found that the numerical results were in good agreement with experiments. Future studies are planned to optimize the hull vane design and orientation for better efficacy
Keywords: Resistance, CFD, Coefficient of Total Resistance, Hull Vane

1. Introduction:

In the present scenario, for the development of an area or country, the mode of transportation is an important aspect. Sea transportation has an important function in various practical applications such as defense, tourism, and economical sectors. To accommodate these needs, a high-speed ship is necessary to fulfil these areas. With increasing requirements for environmental protection, the International Maritime Organization (IMO) has prescribed mandatory regulations such as Energy Efficiency Design Index (EEDI), Energy Efficiency Existing Ship Index (EEXI), and Energy Efficiency Operation Index (EEOI). Resistance of the vessel is one of the predominant complications which is always there for high-speed ships when sailing in the sea, which in turn leads to emissions and reduces the ship's speed. Resistance analysis of the ship is a foremost aspect of ship design.

The main focus of this study is to reduce the resistance of the ship because of the hull vane. Hull vane is a fixed foil that is attached at the transom of the vessel, below the water surface, oriented horizontally in the lateral direction. The hull vane was invented by Doctor Peter Van Oossanen in 1992 and patented in 2002. The flow around the hull vane develops an additional thrust due to the angle between the water inflow and the chord line, resulting in a net force in the forward direction. Furthermore, the low-pressure region on the top surface of the hull vane reduces the generation of waves, and the lift force generated by the hull vane reduces the trim by the stern and the vessel's motions in waves, leading to resistance reduction and saving of fuel and a higher comfort level for the crew and passengers.

Author's Biography

Goutham S is a Research scholar, at Indian Institute of Technology Madras, pursuing research in the field of Ship Hydrodynamics with respect to the application of Hull Vane Technology in Hydrodynamic Drag Reduction of Ships. He has a background in both Mechanical Engineering and Ocean Engineering and led several major projects in the field of Computational Fluid Dynamics. He worked as a Project Scientist at National Institute of Ocean Technology Chennai. He can be reached at gouthamaarya9@gmail.com.

Cdr (Dr) R Vijayakumar (Retd.) is a PhD from Indian Institute of Technology Delhi. He is presently working as an Associate Professor at Department of Ocean Engineering at Indian Institute of Technology, Madras. His fields of interest include warship design, submarine design, ship hydrodynamics, ship dynamics and computational fluid dynamics, green ship technologies and autonomous under water vehicles. Current research was entirely undertaken under his guidance. He can be reached at vijay2028@iitm.ac.in.

The hull vane was successfully applied to a 55 m *MV Karina* fast supply vessel and a 42 m *Alive* superyacht was reported (V & V, 2002). When hull vane was Applied to a 108 m Holland-class OPV, a reduction in total fuel consumption up to 12.5% was reported (Bruno Bouckaert et al., 2015). Other advantages consist of lower vertical acceleration at the helicopter deck, increased sailing range, and increased top speed (B. Bouckaert et al., 2016).

A better seakeeping performance, reduced pitch motion, and added resistance were reported due to the application of a hull vane to a Ro-pax vessel (Uithof, Bouckaert, et al., 2016). The Numerical performance prediction comparison of a hull vane, Interceptor, Trim wedges, and Ballasting were compared in a study to an AMECRC #13 high-speed displacement vessel (Uithof, Hagemeister, et al., 2016). It was found that the Hull Vane was the most efficient device in reducing the ship resistance and improving the seakeeping performance. For this vessel, the position of the hull vane was varied in the vertical and longitudinal directions. They reported the maximum resistance reduction up to 32.4% between 0.2 and 0.8 Froude number for hull vane's position with leading-edge approximately 2.5 chord lengths behind the transom and reduction in vessel's trim by stern and sinkage. The horizontal position of the hull vane played a more significant role than the vertical position of the hull vane.

Considering the positions of the hull vane in vertical and longitudinal directions relative to the ship hull, it is recommended that it should not be placed too close to the hull. On the other hand, it also should not be placed too far below the hull as the angle of attack from the water is decreased. In most applications, it should be placed aft of the transom and not too close to the free surface (V & V, 2002). these results are verified and reported for the crew boat that the position of the most effective vane in the vertical direction was h/T = 0.75 (Suastika et al., 2017). Furthermore, the analysis of the crew boat reported that there was a 10% reduction of resistance and the hull vane was effective in the Froude number ranges between 0.5 and 0.7.

Studies on the hull vane based on CFD simulations and model tests have been reported previously where the device was applied to different types of vessels, such as sailing yachts, motor yachts, supply vessels, container ships, cruise ships, and ro-ro vessels. It was found that the hull vane was only suitable in certain applications (Supply Vessels, ferries, patrol vessels), not in all cases (Bulk carriers and crude oil carriers), since in some applications a resistance increase was found. The buttock angle, the transom submergence, and the stern form significantly determine the hull vane's performance (V & V, 2002). It is also reported that hull vane is more effective between the Froude numbers 0.2 to 0.7.

This study aims to investigate the effect of the hull vane which is retrofitted to a high-speed displacement vessel in 1:35 scale with different locations and angle of attack. The numerical study was carried out using Reynolds Averaged Navier Stokes equation (RANS) based Computational Fluid Dynamics (CFD) on Froude number ranges between 0.2 – 0.42. It has been found sinkage and trim have reduced significantly up to 20 percent along with the drag of the vessel. For validating the present numerical study, towing tank experiments were carried out and compared. It was found that the numerical results were in good agreement with the experiments.

2. Methodology

The vessel chosen for the study is a high-speed displacement vessel (operating Fn = 0.17-0.45) with a length of 142 m with a transom stern. The experimental model with a scale ratio is 35 was prepared. The main particulars of the ship and model are listed in Table 1. The experimental and numerical studies were conducted between 0.17 and 0.45 Froude numbers. The foil used for hull vane is NACA 4412 which is extensively used in the literature ((Sm et al., 2016), (Budiyanto et al., 2020), (Hou et al., 2020), and (Aria & Utama, 2021)). The particulars of the hull vane for the validation study are listed in Table 2. For this study, the chosen span of the hull vane is 9.3% of the length of the water line (*Lwl*) of the vessel which is equal to the width of the transom and the chord of the hull vane is 1.24% of the *Lwl* of the vessel. The hull and hull vane are shown in Figure 1.

Table 1: Main Particulars of high-speed Displacement vessel

Particulars	Model	Prototype	Units
LOA	4.05	142.08	m
Breadth (B)	0.480	16.80	m
Draft (T)	0.123	4.30	m
Wetted Surface Area	1.680	2058	m^2
Lwl	3.871	135.45	m
Displacement (Δ)	110.74	4881.320	Kg/tonnes
Froude Number	0.17-0.45 (12kn-32kn)		

Table 2: Main Parameters of hull vane

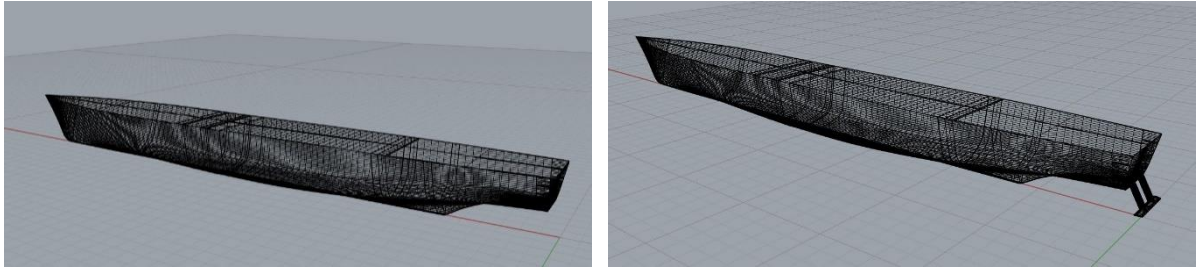| Particulars	Dimension
Angle of the hull vane	0 Deg
Chord	1.24 % of LwL
Span	9.30 % of LwL
X	0.90 % of LwL from Transom Edge
Y	4.07 % of Draft (T) from Transom Edge

Figure 1: CAD model of high-speed Displacement model vessel with and without hull vane

2.1. *Variation of Hull vane position*

To arrive at the optimum location (both longitudinal and depth) of the hull vane at the aft of the vessel for greater resistance reduction, nine locations have been chosen for the present study. The location of the hull vane with respect to the stern edge is shown in Figure 2 and tabulated in Table 3. The first position named HV1 is at 15 mm behind the transom bottom edge in the X-direction, and 5 mm, below the transom bottom edge in Z-direction. The remaining hull vane positions in X-direction and Z-direction are staggered as listed in table 3. A numerical study for all the cases has been carried out, and the resistance of the vessel with and without the hull vane is compared at a cruising speed of 0.37 Fn. All other parameters like foil angle, span, and chord are kept unchanged. The angle of the foil (Angle between the chord line and body-fixed X-axis) is considered as 2 degrees and the span of the foil is equal to transom width.

Table 3: Variation of hull vane's position

Model	Position of foil from transom edge (mm)		Foil dimension in % of L_{wl}	
	X Position	Z Position	Span	Chord
HV1	-15	-3.76	9.3	1.24
HV2	-15	-8.76	9.3	1.24
HV3	-25	-8.76	9.3	1.24
HV4	-25	-3.76	9.3	1.24
HV5	-35	-3.76	9.3	1.24
HV6	-35	-8.76	9.3	1.24
HV7	-35	-13.76	9.3	1.24
HV8	-25	-13.76	9.3	1.24
HV9	-15	-13.76	9.3	1.24

Table 4: Main Parameters of hull vane

Parameter	Settings
Solver	3D Stationary, Unsteady, Implicit
Turbulence Model	Realisable κ-ε
Wall Treatment	Two-layer all wall y+ treatment
Multiphase Flow Model	Volume Of Fluid (VOF), Gravity
Pressure discretization	Standard
Momentum discretization	Second order upwind
Time discretization	First order upwind
Turbulent kinetic energy discretization	Second order upwind
Turbulence dissipation rate	Second order upwind
Pressure-Velocity coupling	SIMPLE
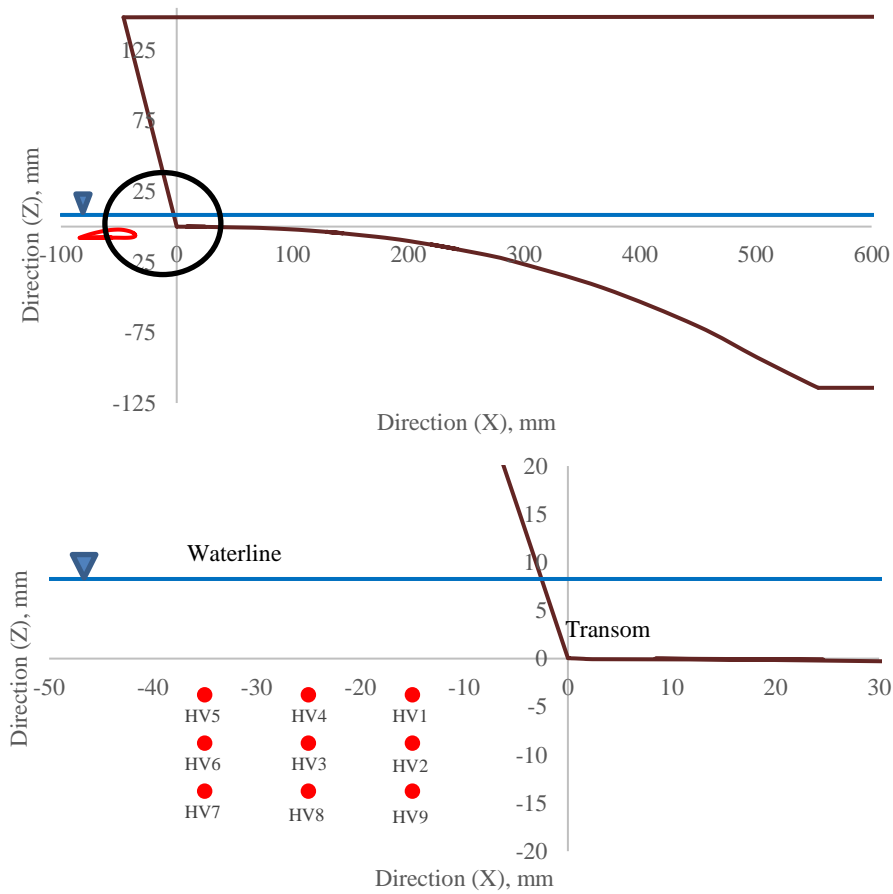
Figure 2: Position of hull vane variation in X and Z-direction

2.2. *Domain Geometry*

To capture the flow phenomenon the domain boundaries around the hull form in all three directions including the air space must conform to sufficient distances. The domain conforms to those recommended in the literature and also with the recommendations of the International Towing Tank Conference (ITTC) namely, ITTC 7.5-03-02-03. As per these standards, the computation grid extends to 2L (where L is the length of the ship) in front of the ship, 3L behind the transom, and 2L above the hull deck, below the keel, and to the sides of the hull. The domain dimensions are shown in Figure 3. Due to the centreline symmetry of the ship as well as to reduce the computational effort, the only half domain is considered. The normal velocity and the normal gradients of all the variables are zero at the symmetry plane and the analysis process considers the dynamic trim based on the two degrees-of-freedom motions in the vertical plane along the hull (Suneela et al., 2021).
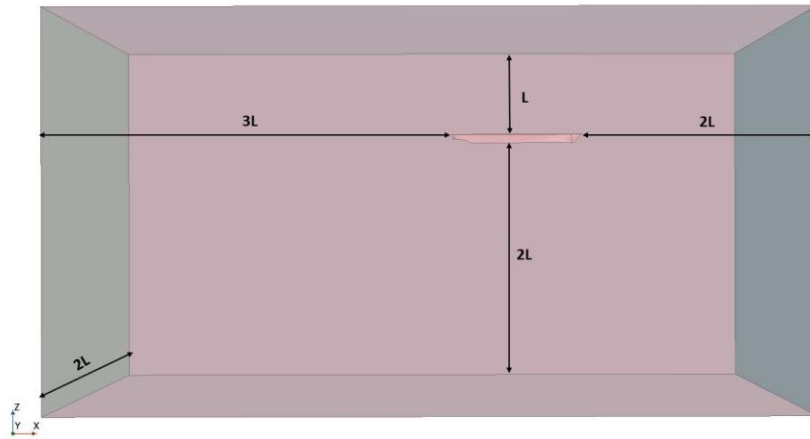
Figure 3: Domain dimensions for CFD simulations

2.3. Meshing

The computational domain is discretized by employing a finite volume approach with trimmed hexahedral control volumes, containing mostly hexahedral cells with trimmed hex cells near a surface to capture the curvature. The multi-zone unstructured grid has been used for domain discretization, for this, the complete flow domain is discretized into zones. These zones are further discretized with hexahedral cells. To reckon the pressure and hence the forces caused by wave making a multiphase flow model volume of fluid (VOF) and Gravity model are employed. Ten prism layers are generated adjoining the hull surfaces to capture boundary layer flow precisely. The cell parameters in prism layer mesh are chosen based on the Wall y+ requirement for proper turbulence modeling. In order to get the high y+ wall treatment which is recommended range for wall function application is kept between 30 and 100 for the near wall y+ treatment. The strategy adopted is to have fine mesh near the body and at the free surface to capture all flow variation and progressively coarser mesh away from the body as shown in Figure 4. Thus, the mesh domain modeled for resistance calculation of high-speed Displacement vessel has 2.6 million cells without HV and 4.1 million with HV.
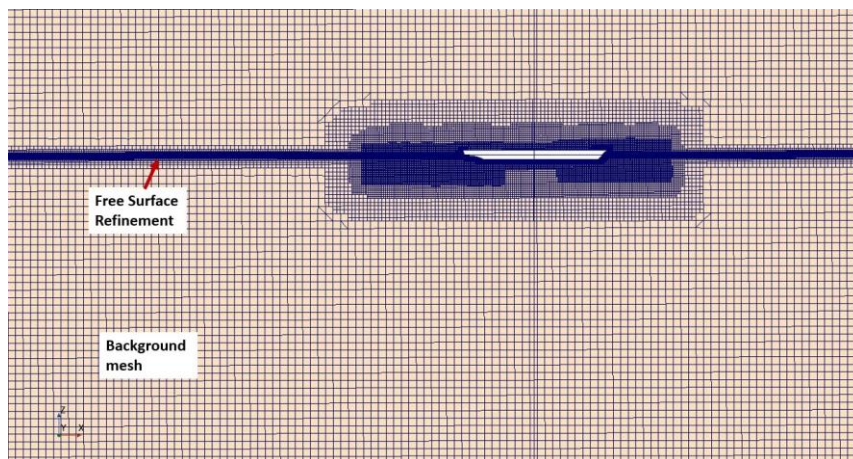

Figure 4: Free Surface Refinement & Background mesh

2.4. CFD Setup

Water and air are described as current and wind speed, respectively, in directions counter to the ship's speed. The ship speed in the simulation is used as the constant value for the inlet velocity. A no-slip boundary condition is applied to the surface body (ITTC, 2017). The boundaries at the inlet, side (both sides if we consider full vessel for analysis, bottom, and top are regarded as the velocity inlet. Pressure is taken to exit at the outlet boundary (ITTC, 2017).

The free surface is the boundary between air and water that meets the physics of flow in both a kinematic (no flow crosses the wave surface) and dynamic (normal stresses balance the ambient atmospheric pressure) manner (ITTC, 2017). In the Navier-Stokes equation, the pressure variable has no equation to be solved. Therefore, it is

necessary to indirectly estimate the pressure using the continuity equation. The segregated flow solver, which uses a pressure-velocity coupling, is used in the pressure study. The governing equations are solved individually by the segregated approach known as the Semi-Implicit Method for Pressure Linked Equations (SIMPLE).

The shear stress on the model scale ship hulls computed using the K-Epsilon turbulence model with wall functions is more accurate when the Wall Y+ of the hull underwater is ~5, (Azcueta 2000). All the simulations are performed using an implicit unsteady solver with a κ-ε turbulence model. The realizable k–ε turbulence model is generally used in most ship flow applications and ITTC (2014) reported that there is not much difference when compared with the k–ω model.

2.5. *Experimental Setup*

The model high-speed displacement vessel is subjected to towing tests in accordance with the ITTC-recommended procedure 7.5-02-05-01 for high-speed Marine Vehicles (HSMV) resistance test, which is based on the 2002 prediction technique. The towing tank at IIT Madras (Member IITC) is 82 meters in length, 3.2 meters in width, and 2.5 metres deep. The towing tank carriage is only capable of 4 m/s of top speed. Two pivot levers and a brake pad were used to mount the high-speed displacement vessel model to the towing carriage. To mitigate the impact of surge, sway, yaw, and roll motions, the model is constrained. The only motions the model was permitted to have were pitch and heave.

Figures 5 and 6 display the model created from the parent hull. Based on hydrodynamic considerations, the model was taken into account at a 1:35 scale. At the vessel's tow point, a standard 50 kg load cell was used to monitor the model's drag forces, and a motion reference unit (MRU) was used to measure trim angles constantly throughout time. On the same scaled model, the numerical analysis was carried out. Table 1 lists the main characteristics of the model craft. The experimental findings from the towing tank at IIT Madras serve to corroborate the numerical calculations. The view of the experiment-use hull and hull vane is depicted in Figures 5 and 6.
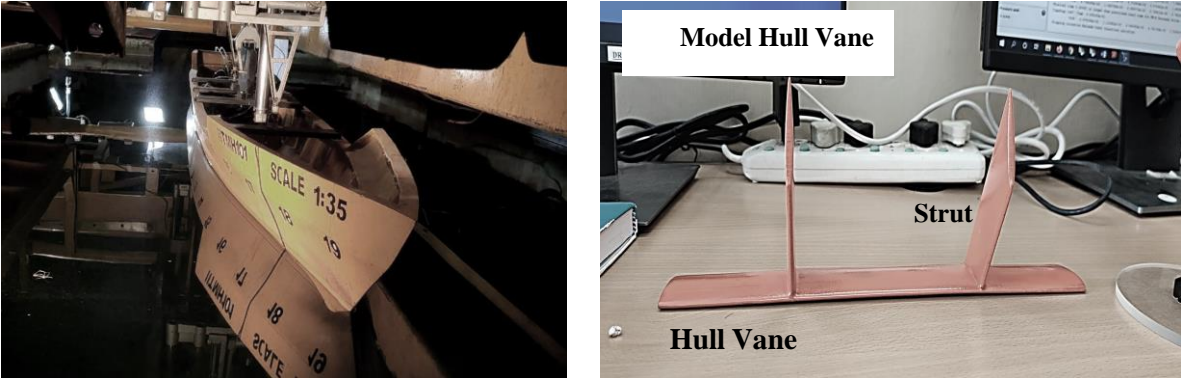

Figure 5: hull model and hull vane

Figure 6: Experimental setup and experiment in progress

3. CFD Validation Case Study

The simulations have been carried out using the RANSE-based commercial package Star-CCM+ to find out the resistance of the model at even keel condition at 0.123 m model draft (this has involved 12 simulations for speed range from 10 knots to 30 knots in steps of 2 knots) for the bare hull. To validate the predicted results from the CFD, experiments have been done for the same speed range and a draft of the vessel for the model scale.

3.1. Grid Independency Study

Grid independency study is carried out for 5 different mesh conditions and at a Froude number of 0.34. The results are tabulated in Table 5 and are plotted in Figure 7. Initially, the base size of 1 m of mesh condition for generated domain and fine mesh near the free surface and around the hull is taken, which results in 1.7 M cells. With respect to base size 1 m, for the remaining iterations, the base size was taken such as 1.414, 1.202, 0.85, and 0.707 m was taken into consideration for the grid independency study. These base sizes result in coarser to finer mesh conditions respectively. For all the mesh conditions, the variation with respect to the base size of 1 m is less than 1 % has been observed.

Table 5: Grid independency study at Froude number 0.34

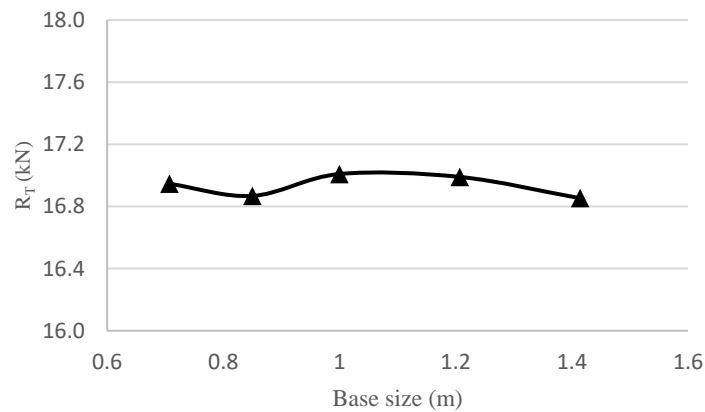| Base Size	Resistance (N)	% Deviation of Resistance
1.414	16.85	0.91
1.207	16.99	0.11
1	17.01	0.00
0.85	16.87	0.83
0.707	16.95	0.37

Figure 7: Grid independency study (Resistance of the model at Froude number 0.34 vs Base size)

3.2. Validation of Numerical Results for Bare Hull

Figure 8 displays a comparison chart of the resistance experienced by the bare hull when the CFD and Experiments are conducted. The simulations are carried out for the range of velocities for the chosen mesh conditions and it is plotted in Figure 8. The predicted results from CFD simulations are compatible with the experimental results which are obtained from the towing tank test. The results indicate that the deviations are within the range of 2 – 5% for the speed range of 0.2 to 0.45 Fn. The deviation is up to 5% when speed goes near the 0.4 Froude number as shown in Figure 8. The red-colored numbers in the graph indicate that the percentage deviation of CFD results from the experimental results with respect to the respective Froude number.
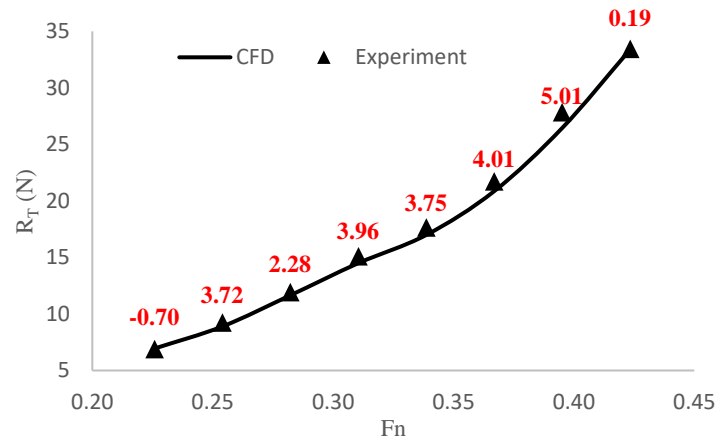
Figure 8: Comparison of CFD results with the experimental results for bare hull with respect to Froude number

3.3. Validation of Ship resistance with Hull vane

The experiments have been conducted for hull with hull vane in the towing tank. The hull vane span is 8.27% of the *Lwl* of the ship, the Chord of the hull vane is 1.24% of the *Lwl* of the ship, and it is placed away from the hull transom edge in the vertical direction of the hull vane.

The experimental findings from the towing tank available at IIT Madras, which are depicted in Figure 9, validate the projected results from numerical models for three speeds. Deviation of Predicted results from the experimental is around 4%
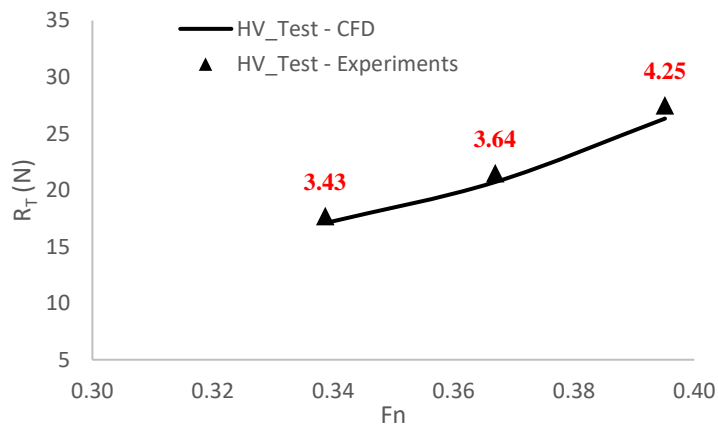.

Figure 9: Validation of hull with hull vane for three different Froude number

4. Results & Discussions

Numerical analysis and model test of the bare hull and hull fitted with hull vanes were carried out and presented for Froude numbers 0.17-0.45, where a validation study is conducted. The configurations at which the numerical study is conducted are listed in Table 3. The numerical solution for the present study is to identify the configuration at which the vessel is showing better performance characteristics at the Froude number of 0.37. Table 6 displays that the configuration HV5 shows less resistance than all the other configurations. For the HV5 arrangement, the low-pressure area on the upper surface of the hull vane is favourably interfering with the wave system since it is situated close to the rooster tail. Thereby energy lost to the ships is less in this case. It is also indicating that when the hull vane is near the transom of the model, there is less reduction in the resistance of the vessel.

To study the effect of foil angle on the wave height at the stern portion of the vessel, the HV5 case has been selected for further analysis, the angle of the hull vane has been varied from 2º to 0º, 5º and 10º. The reduction in resistance is more at the 0º foil angle. Therefore, further CFD simulations have been carried out for all the Froude numbers ranging from 0.2 to 0.42 to see the effect of the hull vane at every speed.

Table 6: CFD simulation results for various hull vane configurations conduced

Hull Vane	Resistance (N)	% Deviation from bare hull
HV1	20.84	-0.10
HV2	20.48	-1.82
HV3	20.44	-2.01
HV4	20.45	-1.97
HV5	20.23	-3.02
HV6	20.27	-2.83
HV7	20.32	-2.59
HV8	20.38	-2.30
HV9	20.30	-2.68

A comparison plot of the total resistance coefficient and the total residual resistance coefficient of the bare hull and the hull with the hull vane with a variation in the Froude number is shown in Figures 10 and 11.

The resistance coefficient is calculated as

$$C_T = \frac{R_T}{\frac{1}{2}\rho V^2 A}$$

Where R_T is the total ship resistance, ρ is the mass density of water, V is the ship speed, and A is a wetted surface area (WSA). Based on the predicted numerical results, it can be said that the installation of the hull vane to the model high-speed displacement vessel was able to reduce the total resistance coefficient (C_T) by 6% and total residuary resistance coefficient (C_R) by 20.81%. The reduction in C_R was compensated by the increase in the total frictional resistance coefficient (C_F). this increase in C_F is because of increase in the wetted surface area (WTA) of the hull vane which is added to the wetted surface area of the vessel. Further, CFD simulations indicate that the reduction in resistance coefficient C_T or C_R is more when the Froude number/ship speed is increasing. When the Froude number is less than 0.2, the coefficient of resistance of the hull with the hull vane case is not smaller than the bare hull case. When the Froude number is greater than 0.2, the coefficient of resistance due to the installation of the hull vane is smaller than the bare hull case (V & V, 2002).
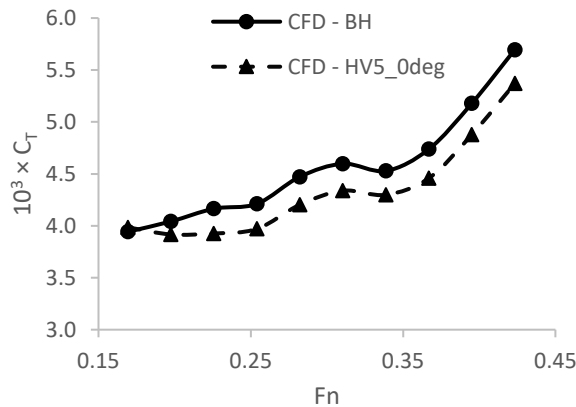

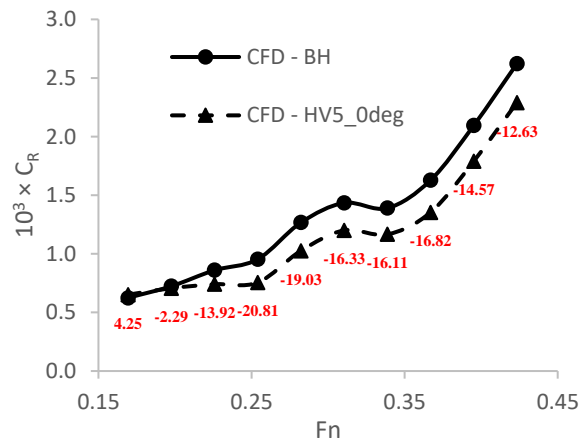Figure 10: Coefficient of the total ship resistance (C_T) as a function of the Froude number (Fn)

Figure 11: Coefficient of the reisduary resistance (C_R) as a function of the Froude number (Fn)

To analyse the impact on motion and the cause of resistance reduction, the analytical process additionally takes into account the dynamic trim based on the two degrees-of-freedom motions (Trim & Sinkage) in the vertical plane along the hull. The trim response of the model, shown in degrees at all speeds, is shown in Figure 12. Trim by stern is represented by the negative symbol (which means downward movement of the bow). The model vessel for the bare hull case exhibits trim by the stern reaction for all speed ranges, and the trim of the model increases as the Froude number increases. The largest trim can reach -0.58 deg at 0.42 Froude number. When the hull vane

was installed, the trim of the vessel decreases to 0-0.23 at 0.42 Froude number due to the vertical force on the hull vane by the fluid. This change in trim (decrease in trim) due to the installation of the hull vane is not identical for every speed which is less at the lesser Froude numbers, and more at the higher Froude numbers. It can be seen in Figure 9 that, the trim of the vessel changes to trim by bow due to the installation of the hull vane in between the Froude numbers 0.25 to 0.37 (which is the operating Froude number range in the sea).

Meanwhile, Figure 13 indicates the sinkage generated by the bare hull model and model with the hull vane. It can be seen from Figure 13 that; the sinkage of the vessel increases with increasing the Froude number for both the cases. Sinkage causes an increase in draft and wetted surface area of the vessel, which leads to an increase in the total resistance. Due to the installation of the hull vane, the sinkage of the vessel is lesser than the sinkage of the bare model hull case which is because of the vertical force on the hull vane by the fluid. hull vane helps in reducing the sinkage of the vessel, but the difference is minimal up to 10%.
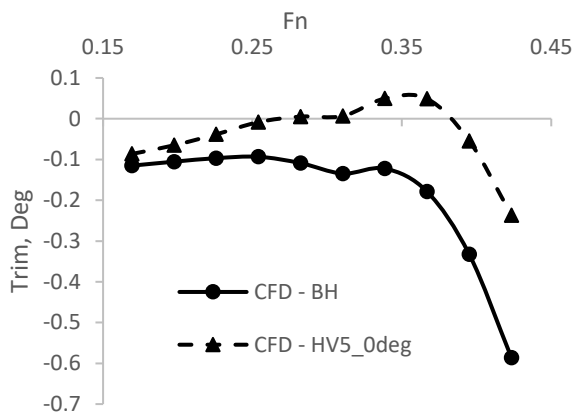

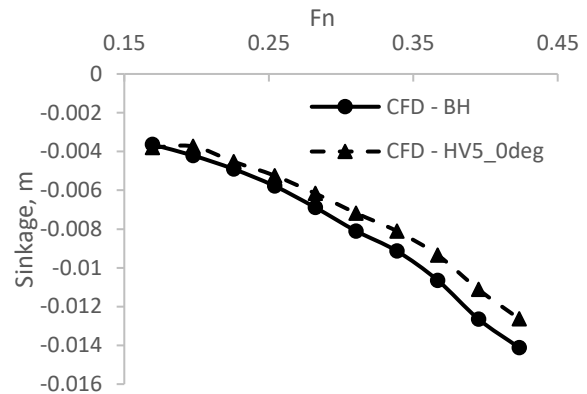Figure 12: Trim of the vessel as a function of the Froude number (*Fr*)

Figure 13: Sinkage of the vessel as a function of the Froude number (*Fr*)

The hull vane plays a major role in a stern wave pattern of the wave system by creating a low-pressure region behind the transom of the vessel. This low pressure is due to the high velocity on the top surface of the hull vane. this low-pressure region behind the transom of the vessel interacts favorably with the stern wave pattern, thereby reducing the wave-making resistance of the ship. Figure 14 indicates wave height/*Lwl* behind the transom to the *X/Lwl*. It can be seen from the plot that just behind the transom there is a low-pressure region that is absorbing the stern wave system resulting in the reduction of the wave energy lost to the ship. The residuary coefficient of resistance is reduced by 21% but which is compensated by the frictional resistance added to the ship due to the hull vane's wetted surface area.
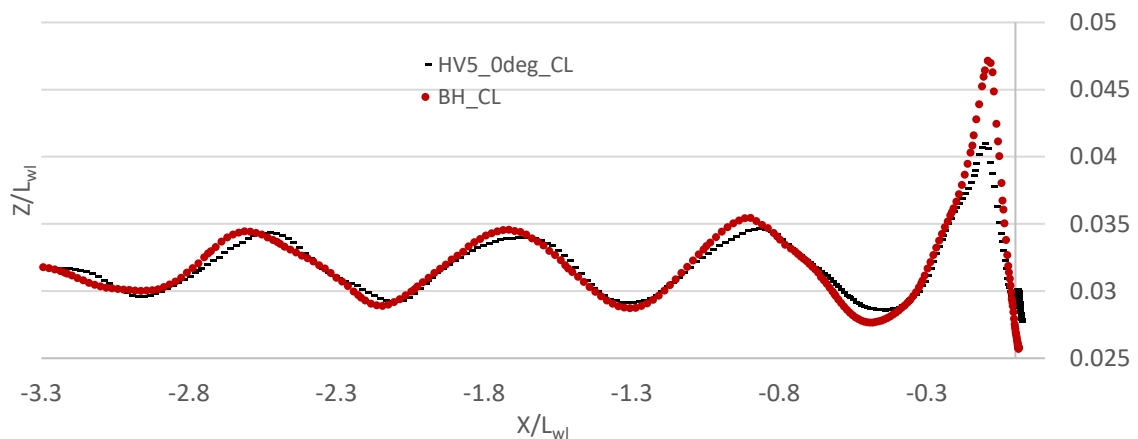

Figure 14: The wave height/L_{wl} for bare hull and hull with hull vane at Froude number 0.37

5. Conclusions

Based on experiments and numerical simulations that have been carried out, it is observed that the CFD simulation results and experimental results were agreeable with each other for the bare hull and hull vane cases. CFD simulations have been carried out by installing different locations and orientation of the hull vane and it has been found that the hull vane should not be placed very closed and far away from the hull (the vertical direction Z-direction). It is also found that the total resistance coefficient is decreased up to 6% and the residuary coefficient of resistance decreased by 20.81% for best location. Even though there is a decrease in C_R of 20.81%, it is observed that, there is a marginal increase in the wetted surface area results in increase frictional resistance, hence the overall decrease in C_T is around 6%. The trim and sinkage of the vessel have been reduced by 20%.

In future studies, the effect of variation in the span of the hull vane and self-propelled CFD simulations will be performed with enhanced hull vane shape to see the effect of hull vane on real conditions.

Acknowledgements

References

Uithof, K., Van Oossanen, P., Moerke, N., Van Oossanen, P. G., & Zaaijer, K. S. (2014, December). An update on the development of the Hull Vane. In *9th International Conference on High-Performance Marine Vehicles (HIPER), Athens* (pp. 211-221).

Bouckaert, B., Uithof, K., van Oossanen, P., Moerke, N., Nienhuis, B., & van Bergen, J. (2015, September). A life-cycle cost analysis of the application of a Hull Vane to an Offshore Patrol Vessel. In *SNAME 13th International Conference on Fast Sea Transportation.* OnePetro.

Andrews, I., Avala, V. K., Sahoo, P. K., & Ramakrishnan, S. (2015, September). Resistance characteristics for high-speed hull forms with vanes. In *SNAME 13th International Conference on Fast Sea Transportation.* OnePetro.

Uithof, K., Hagemeister, N., Bouckaert, B., Van Oossanen, P. G., & Moerke, N. (2016). A systematic comparison of the influence of the Hull Vane®, interceptors, trim wedges, and ballasting on the performace of the 50m AMECRC series# 13 patrol vessel. *Proc. Warship.*

Bouckaert, B., Uithof, K., Moerke, N., & Van Oossanen, P. G. (2015, September). Hull Vane on 108m Holland-Class OPVs: Effects on Fuel Consumption and Seakeeping. In *Proceeding of MAST Conference.*

Uithof, K., Bouckaert, B., Van Oossanen, P. G., & Moerke, N. (2016). The effects of the Hull Vane® on ship motions of ferries and RoPax vessels. *RINA Design & Operation of Ferries & Ro-Pax Vessels, London.*

Hagemeister, N., Uithof, K., Bouckaert, B., & Mikelic, A. (2017, September). Hull Vane® versus Lengthening, a comparison between four alternatives for a 61 m OPV. In *FAST Conference.*

Suastika, K., Hidayat, A., & Riyadi, S. (2017). Effects of the application of a stern foil on ship resistance: A case study of an Orela crew boat. *International Journal of Technology*, *8*(7), 1266-1275.

Bouckaert, B. (2018). An underwater spoiler on a warship: why, when and how?. *Zeszyty Naukowe Akademii Marynarki Wojennej*, *59.*

Ferreé, H., Goubault, P., Yvin, C., & Bouckaert, B. (2019). Improving the nautical performance of a surface ship with the Hull Vane® appendage. *Association Technique Maritime et Aéronautique. Numéro*, *2738.*

Celik, C., Danisman, D. B., Kaklis, P., & Khan, S. (2019). An investigation into the effect of the Hull Vane on the ship resistance in OpenFOAM. In *Sustainable Development and Innovations in Marine Technologies* (pp. 136-141). CRC Press.

Budiyanto, M. A., Murdianto, M. A., & Syahrudin, M. F. (2020). Study on the resistance reduction on high-speed vessel by application of stern foil using cfd simulation. *CFD Letters*, *12*(4), 35-42.

Hou, H., Krajewski, M., Ilter, Y. K., Day, S., Atlar, M., & Shi, W. (2020). An experimental investigation of the impact of retrofitting an underwater stern foil on the resistance and motion. *Ocean Engineering*, *205*, 107290.

Budiarto, U., & Firdhaus, A. (2021, February). Analysis of the effect of hull vane on ship resistance using CFD methods. In *IOP Conference Series: Earth and Environmental Science* (Vol. 649, No. 1, p. 012051). IOP Publishing.

Suneela, J., Krishnankutty, P., & Anantha Subramanian, V. (2020). Numerical investigation on the hydrodynamic performance of high-speed planing hull with transom interceptor. *Ships and Offshore Structures*, *15*(sup1), S134-S142.

Campana, E., Gorski, J., Chun, H., Day, A., Huang, D., MacFarlane, G. J., ... & Valle, J. (2008). The Resistance Committee-Final Report and recommendations to the 25th ITTC. In *25th International Towing Tank Conference* (Vol. 1, pp. 1-61).

Sindagi, S., Vijayakumar, R., & Saxena, B. K. (2020). Parametric CFD investigation of ALS technique on reduction in drag of bulk carrier. *Ships and Offshore Structures*, *15*(4), 417-430.

Sindagi, S., & Vijayakumar, R. (2021). Succinct review of MBDR/BDR technique in reducing ship's drag. *Ships and Offshore Structures*, *16*(9), 968-979.

Sindagi, S., Vijayakumar, R., & Saxena, B. K. (2018). Frictional drag reduction: Review and numerical investigation of microbubble drag reduction in a channel flow. *International Journal of Maritime Engineering*, *160*(A2).

Hemanth Kumar, Y., & Vijayakumar, R. (2020). Effect of flap angle on transom stern flow of a High speed displacement Surface combatant. *Ocean Systems Engineering*, *10*(1), 1-23.

Kumar, Y. H., & Vijayakumar, R. (2020). Development of an Energy Efficient Stern Flap for Improved EEDI of a Typical High-speed Displacement Vessel. *Defence Science Journal*, *70*(1).

Sindagi, S., Vijayakumar, R., Nirali, S., & Saxena, B. K. (2019). Numerical investigation of influence of microbubble injection, distribution, void fraction and flow speed on frictional drag reduction. In *Proceedings of the Fourth International Conference in Ocean Engineering (ICOE2018)* (pp. 293-318). Springer, Singapore.

Hemanth Kumar, Y., & Vijayakumar, R. (2018). Stern flaps: A cost-effective technological option for the Indian shipping industry. *Maritime Affairs: Journal of the National Maritime Foundation of India*, *14*(2), 26-37.

Subramanian, V. A., & Vijayakumar, R. (2006). An inverse design approach for minimising wake at propeller plane using CFD. *Ocean engineering*, *33*(2), 119-136.

Sindagi, S., Vijayakumar, R., & Saxena, B. K. (2021). Experimental parametric investigation to reduce drag of a scaled model of bulk carrier using BDR/ALS technique. *Journal of Ship Research*, *65*(03), 257-265.

Sindagi, S., Vijayakumar, R., & Saxena, B. K. (2021). Experimental investigation on ship's model in carrying out energy economics of BDR/ALS methodology. *Ships and Offshore Structures*, 1-10.

Hemanth Kumar, Y., & Vijayakumar, R. (2021). Experimental Studies of Stern Flap Performance on a Transform Stern High-Speed Displacement Vessel. In *Proceedings of the Fifth International Conference in Ocean Engineering (ICOE2019)* (pp. 529-540). Springer, Singapore.

Kumar, Y. H., & Vijayakumar, R. (2022, February). Experimental Analysis of Stern Flap Effects on the Pressure Distribution at Transom Stern. In *OCEANS 2022-Chennai* (pp. 1-5). IEEE.

Sindagi, S., & Vijayakumar, R. (2022, February). The Energy Economics of Air Lubrication System. In *OCEANS 2022-Chennai* (pp. 1-10). IEEE.

Gokulakrishnan, M., Kumar, A., & Vijayakumar, R. (2022, February). Numerical Estimation of Frictional Drag on Flat Plate In Shallow Water with & without BDR. In *OCEANS 2022-Chennai* (pp. 1-7). IEEE.

Gokulakrishnan, G., Kumar, A., & Vijayakumar, R. (2022, February). Numerical prediction of hydrodynamic forces and moments of KCS in shallow water. In *OCEANS 2022-Chennai* (pp. 1-7). IEEE.

Vipin, C. V., Gopinath, S., & Vijayakumar, R. (2022, February). Numerical Study on A Planning Hull to Improve the Sea Water Intake at High Speed. In *OCEANS 2022-Chennai* (pp. 1-8). IEEE.

Nimmagadda, N. V. R., Polisetty, L. R., & Vaidyanatha Iyer, A. S. (2020). Simulation of air–water interface effects for high-speed planing hull. *Journal of Marine Science and Application*, *19*(3), 398-414.